

Galaxies with Supermassive Binary Black Holes: (I) A Possible Model for the Centers of Core Galaxies

Ing-Guey Jiang¹ and Li-Chin Yeh²

¹ *Department of Physics and Institute of Astronomy,
National Tsing-Hua University, Hsin-Chu, Taiwan*

² *Department of Applied Mathematics,
National Hsinchu University of Education, Hsin-Chu, Taiwan*

jiang@phys.nthu.edu.tw

ABSTRACT

The dynamics of galactic systems with central binary black holes is studied. The model is a modification from the restricted three body problem, in which a galactic potential is added as an external potential. Considering the case with an equal mass binary black holes, the conditions of existence of equilibrium points, including Lagrange Points and additional new equilibrium points, i.e. Jiang-Yeh Points, are investigated. A critical mass is discovered to be fundamentally important. That is, Jiang-Yeh Points exist if and only if the galactic mass is larger than the critical mass. The stability analysis is performed for all equilibrium points. The results that Jiang-Yeh Points are unstable could lead to the core formation in the centers of galaxies.

1. Introduction

A modification of the restricted three body problem was first studied in Chermnykh (1987). The angular velocity variation of the system was considered and the stability of solutions near equilibrium points was investigated. Extending from the work of Chermnykh (1987), Papadakis (2004) studied the symmetric motions near the three collinear equilibrium points, Papadakis (2005a) investigated the stability of the periodic orbits and explored the network of the orbital families, Papadakis (2005b) provided the analytic determination of the initial conditions of the long- and short-period Trojan families around the equilibrium points of the Sun-Jupiter system.

Then, Jiang & Yeh (2006) and Yeh & Jiang (2006) investigated the existence of new equilibrium points of a system with binary masses and a disk as a modification of the restricted

three body problem, which was hereafter called Chermnykh-like problem for convenience (Jiang & Yeh 2006, Yeh & Jiang 2006). Moreover, Kushvah (2008a, 2008b, 2009) studied the linear stability of equilibrium points of the generalized photo-gravitational problem. The trajectories and Lyapunov characteristic exponents are also calculated and studied in Kushvah (2011a, 2011b).

Furthermore, the recent rapid development of the discoveries of extra-solar planetary systems has triggered many interesting theoretical work (see Jiang & Ip 2001, Ji et al. 2002, Jiang et al. 2003, Jiang & Yeh 2004a, Jiang & Yeh 2004b, Jiang & Yeh 2004c, Jiang & Yeh 2007, Jiang & Yeh 2009, Jiang & Yeh 2011), statistics work (see Jiang et al. 2006, 2007, 2009, 2010), and also the following-up observational work (Jiang et al. 2013) in this field. In fact, some results of the Chermnykh-like problem could have important applications on the dynamical problems of planetary systems (Papadakis 2005b, Kushvah 2011a).

On the other hand, the dynamical evolution of galaxies is another field that Chermnykh-like problems could be used as theoretical models. It is now generally believed that nearly every galaxy hosts a supermassive black hole at the center. It is also believed that most massive elliptical galaxies were formed by merging of existing galaxies. Thus, it is possible that many luminous elliptical galaxies might host binary black holes. The orbital motion of stars near the binary black hole at the centers of galaxies is a dynamical system that Chermnykh-like problems could act as a good model. The possible orbits of these stars would be related with the density profile near the cores of galaxies. The brightness near the core of galaxies does show some signature which might be related with the dynamical evolution of stars near the binary black hole.

For example, Lauer et al. (2007) investigated the cores of early-type galaxies. The detail brightness profiles are systematically classified. However, it is unclear how the cores were formed and how core properties are related with the dynamical evolution of these galaxies. Kandrup et al. (2003) studied the stellar distribution under the influence of a binary black hole and a galactic potential. A systematic transport of stars near the black holes out to larger radii was investigated and the resulting stellar density profile was used to explain the observed profile of NGC 3706.

In order to seek a possible picture to explain the core formation of these early-type galaxies, we here employ a model with a supermassive binary black hole in a galaxy. To analytically understand the dynamical properties of this system, we first investigate the existence of equilibrium points. In addition to the existence of Lagrange points, the conditions under which other equilibrium points would exist are also investigated. After that, the stability of all equilibrium points is discussed.

The model is given in Section 2, the analytic results of equilibrium points are in Section 3, the bifurcation diagrams and locations of equilibrium points are shown in Section 4, the stability analysis is in Section 5, and finally the summary is in Section 6.

2. The Model

We study the dynamical motion of a star near the center of a galaxy. The star, considered as a test particle, is influenced by the galactic potential and the gravitational force from the central supermassive binary black hole (SBBH). Depending on the mass ratio between the galaxy and SBBH, the separation of SBBH, and also the central concentration of the galactic density profile, the central region with SBBH could be dominated by the SBBH, and thus the galactic potential could be ignored approximately. In this case, when the SBBH is moving on circular orbits, the star's equations of motion are exactly as in a restricted three body problem:

(Murray & Dermott 1999, Jiang & Yeh 2006)

$$\left\{ \begin{array}{l} \frac{d\bar{x}}{dt} = \bar{u} \\ \frac{d\bar{y}}{dt} = \bar{v} \\ \frac{d\bar{u}}{dt} = 2\bar{n}\bar{v} - \frac{\partial U^*}{\partial \bar{x}} \\ \frac{d\bar{v}}{dt} = -2\bar{n}\bar{u} - \frac{\partial U^*}{\partial \bar{y}}, \end{array} \right. \quad (1)$$

where \bar{n} is the central binary's angular velocity,

$$U^* = -\frac{\bar{n}^2}{2}(\bar{x}^2 + \bar{y}^2) - \frac{G\bar{m}_1}{\bar{r}_1} - \frac{G\bar{m}_2}{\bar{r}_2}. \quad (2)$$

The Jacobi integral of the above system is

$$\bar{C}_J = -\bar{u}^2 - \bar{v}^2 - 2U^*. \quad (3)$$

The solution and stability of the above system are well studied (Murray & Dermott 1999). In this paper, we are interested in the case with equal mass SBBH, thus we set the mass $\bar{m} = \bar{m}_1 = \bar{m}_2$ and the binary has a separation $2\bar{R}$. Moreover,

$$\bar{r} = \sqrt{\bar{x}^2 + \bar{y}^2}, \bar{r}_1 = \sqrt{(\bar{x} + \bar{R})^2 + \bar{y}^2}, \quad \text{and} \quad \bar{r}_2 = \sqrt{(\bar{x} - \bar{R})^2 + \bar{y}^2}.$$

The equations of motion are now written as:

$$\left\{ \begin{array}{l} \frac{d\bar{x}}{dt} = \bar{u} \\ \frac{d\bar{y}}{dt} = \bar{v} \\ \frac{d\bar{u}}{dt} = 2\bar{n}\bar{v} + \bar{n}^2\bar{x} - \frac{G\bar{m}(\bar{x}+\bar{R})}{\bar{r}_1^3} - \frac{G\bar{m}(\bar{x}-\bar{R})}{\bar{r}_2^3} \\ \frac{d\bar{v}}{dt} = -2\bar{n}\bar{u} + \bar{n}^2\bar{y} - \frac{G\bar{m}\bar{y}}{\bar{r}_1^3} - \frac{G\bar{m}\bar{y}}{\bar{r}_2^3}. \end{array} \right. \quad (4)$$

As the procedure in Yeh, Chen, & Jiang (2012), it is better to do non-dimensionalization for the above system. This would not only simplify equations, but also make it more convenient when we apply mathematical models on real physical systems. When non-dimensional variables are set as

$$x = \frac{\bar{x}}{L_0}, y = \frac{\bar{y}}{L_0}, R = \frac{\bar{R}}{L_0}, t = \frac{\bar{t}}{t_0}, m = \frac{\bar{m}}{m_0}, u = \frac{\bar{u}}{u_0}, v = \frac{\bar{v}}{u_0}, n_b = t_0\bar{n}$$

and some of the above parameters are further assumed as $u_0 = \frac{L_0}{t_0}$ and $Gm_0 = \frac{L_0^3}{t_0^2}$, then System (4) can be rewritten as

$$\left\{ \begin{array}{l} \frac{dx}{dt} = u \\ \frac{dy}{dt} = v \\ \frac{du}{dt} = 2n_b v + n_b^2 x - \frac{m(x+R)}{r_1^3} - \frac{m(x-R)}{r_2^3} \\ \frac{dv}{dt} = -2n_b u + n_b^2 y - \frac{my}{r_1^3} - \frac{my}{r_2^3}, \end{array} \right. \quad (5)$$

where $n_b^2 = \frac{m}{4R^3}$, $r^2 = x^2 + y^2$, $r_1^2 = (x+R)^2 + y^2$, and $r_2^2 = (x-R)^2 + y^2$.

The above are the equations when the galactic potential is ignored in our system. However, in order to generally consider all different masses of the galaxy and SBBH for the study of stellar dynamics near SBBH in the region of a galactic center, the galactic potential shall be included. The Nuker law, which was originally used to characterize the inner light distributions of galaxies (Lauer et al. 1995), is employed to set the overall galactic dark-matter plus luminous density distribution here.

The Nuker law is expressed as

$$\rho(\bar{r}) = \rho_c \left(\frac{\bar{r}}{r_b} \right)^{-\gamma} \left\{ 1 + \left(\frac{\bar{r}}{r_b} \right)^\alpha \right\}^{\frac{\gamma-\beta}{\alpha}}, \quad (6)$$

where $\rho_c, \alpha, \beta, \gamma$ are constants. The scale length r_b is called the break radius. When $\bar{r} \gg r_b$, the above becomes a power law with index β . For $\bar{r} \ll r_b$, γ is the inner cusp slope of this density profile as \bar{r} approaches to zero. Thus, the break radius, r_b , marks a transition from the outer power law with index β to inner cusp with index γ . Usually, the slope of outer

profile is steeper than the central cusp, so that β is larger than γ . Core galaxies are those that exhibit clear break radius but power-law galaxies do not. Both types are studied and classified in Lauer et al. (2007). The properties of central profiles of these two types of galaxies might be related with the general structures and formation histories of galaxies and thus could be fundamentally important. Because the break radius is so important, we set our length scale $L_0 = r_b$ here. In other words, we regard r_b as a typical length scale in our system and we have

$$r = \frac{\bar{r}}{r_b} \quad (7)$$

and a dimensionless Nuker law

$$\rho(r) = \rho_c(r)^{-\gamma} \{1 + (r)^\alpha\}^{\frac{\gamma-\beta}{\alpha}}. \quad (8)$$

According to the observational results and classifications in Lauer et al. (2007), the brightness of galaxies present different values of α, β and γ in the above formula. As a first step, in this paper, we choose $\alpha = 2$, $\beta = 4$ and $\gamma = 0$ (Kandrup et al. 2003). The mass of the galaxy upto a radius r is

$$M(r) = 4\pi \int_0^r r^2 \rho(r) dr = 2\pi \rho_c \left\{ \tan^{-1} r - \frac{r}{1+r^2} \right\}. \quad (9)$$

Note that the mass, potential, radius, and normalization constants etc. are all expressed as dimensionless quantities hereafter for convenience. Obviously, $M(r)$ does not include the mass of SBBH. Thus, if the galactic total mass is M_g , then we have $\rho_c = \frac{M_g}{\pi^2}$.

On the other hand, the corresponding potential is

$$V(r) = -4\pi \left[\frac{1}{r} \int_0^r \rho(\bar{r}) \bar{r}^2 d\bar{r} + \int_r^\infty \rho(\bar{r}) \bar{r} d\bar{r} \right] = -c \frac{\tan^{-1} r}{r}, \quad (10)$$

where $c = \frac{2}{\pi} M_g$. Moreover, from the potential, we can obtain the gravitational force as

$$f_g(r) \equiv -\frac{\partial V}{\partial r} = c \left\{ \frac{1}{(1+r^2)r} - \frac{\tan^{-1} r}{r^2} \right\}. \quad (11)$$

Including this axis-symmetric force into the system, our equations of motion now become:

$$\left\{ \begin{array}{l} \frac{dx}{dt} = u \\ \frac{dy}{dt} = v \\ \frac{du}{dt} = 2nv + n^2x - \frac{m(x+R)}{r_1^3} - \frac{m(x-R)}{r_2^3} + \frac{cx}{r} \left\{ \frac{1}{(1+r^2)r} - \frac{\tan^{-1} r}{r^2} \right\}, \\ \frac{dv}{dt} = -2nu + n^2y - \frac{my}{r_1^3} - \frac{my}{r_2^3} + \frac{cy}{r} \left\{ \frac{1}{(1+r^2)r} - \frac{\tan^{-1} r}{r^2} \right\}. \end{array} \right. \quad (12)$$

Note that the length scale L_0 of the above equations has been set to equal to the break radius r_b of the galaxy we considered in this system. Moreover, under the influence of the galactic potential, the mean motion, i.e. angular velocity, of each component of SBBH in the above equations now becomes

$$n = \left\{ \frac{m}{4R^3} + \frac{1}{R} |f_g(R)| \right\}^{1/2}. \quad (13)$$

The corresponding Jacobi integral of this system is, similar as the one in Jiang & Yeh (2006),

$$C_J = -u^2 - v^2 + n^2(x^2 + y^2) + \frac{2m}{r_1} + \frac{2m}{r_2} + 2c \frac{\tan^{-1}(\sqrt{x^2 + y^2})}{\sqrt{x^2 + y^2}}. \quad (14)$$

3. The Equilibrium Points

It is well-known that there are five equilibrium points, i.e. Lagrange Points, for the classical restricted three-body problem. In the case that when an additional potential is added, the results in Jiang & Yeh (2006) and Yeh & Jiang (2006) show that, two more equilibrium points, called Jiang-Yeh Points hereafter for convenience, might exist under some conditions.

We study the system of equal mass SBBH with galactic potential here. In this paper, the equilibrium point at the origin (0,0) will be named as Lagrange Point 1 (L1), the one at x -axis with $x > R$ is named as Lagrange Point 2 (L2), the one at x -axis with $x < -R$ is named as Lagrange Point 3 (L3), the one at y -axis with $y > 0$ is named as Lagrange Point 4 (L4), the one at y -axis with $y < 0$ is named as Lagrange Point 5 (L5), the one at x -axis with $0 < x < R$ is called as Jiang-Yeh Point 1 (JY1), the one at x -axis with $-R < x < 0$ is called as Jiang-Yeh Point 2 (JY2). In this section, the existence of the above equilibrium points is investigated and the conditions of their existence will be determined and proved.

In general, for System (12), equilibrium points (x_e, y_e) satisfies $A(x_e, y_e) = 0$ and $B(x_e, y_e) = 0$, where

$$A(x, y) = n^2 x - \frac{m(x+R)}{r_1^3} - \frac{m(x-R)}{r_2^3} + \frac{cx}{r} \left\{ \frac{1}{(1+r^2)r} - \frac{\tan^{-1}(r)}{r^2} \right\}, \quad (15)$$

$$B(x, y) = n^2 y - \frac{my}{r_1^3} - \frac{my}{r_2^3} + \frac{cy}{r} \left\{ \frac{1}{(1+r^2)r} - \frac{\tan^{-1}(r)}{r^2} \right\}. \quad (16)$$

For convenience, for $y \neq 0$, we define

$$h(y) \equiv \frac{B(0, y)}{y} = n^2 - \frac{2m}{[R^2 + y^2]^{3/2}} + \frac{c}{|y|} \left\{ \frac{1}{(1+y^2)|y|} - \frac{\tan^{-1}(|y|)}{y^2} \right\}$$

$$= n^2 - \frac{2m}{[R^2 + y^2]^{3/2}} + c \left\{ \frac{1}{(1 + y^2)y^2} - \frac{\tan^{-1}(y)}{y^3} \right\} \quad (17)$$

and then

$$\begin{aligned} k(x) &\equiv A(x, 0) = n^2x - \frac{m(x + R)}{|x + R|^3} - \frac{m(x - R)}{|x - R|^3} + \frac{cx}{|x|} \left\{ \frac{1}{(1 + x^2)|x|} - \frac{\tan^{-1}(|x|)}{x^2} \right\} \\ &= n^2x - \frac{m(x + R)}{|x + R|^3} - \frac{m(x - R)}{|x - R|^3} + c \left\{ \frac{1}{(1 + x^2)x} - \frac{\tan^{-1}(x)}{x^2} \right\} \end{aligned} \quad (18)$$

Because the proofs of Property 3.1 and 3.2 of Jiang & Yeh (2006) does not involve the detail form of the force derived from the additional potential, the result that the equilibrium points are either on the x -axis or y -axis is valid for our system of equal mass SBBH. Besides, we have the following Remarks for our system here.

Remark (A):

For $y_e \neq 0$, y_e satisfies $h(y) = 0$, if and only if $(0, y_e)$ is the equilibrium point of System (12).

Remark (B):

x_e satisfies $k(x) = 0$, if and only if $(x_e, 0)$ is the equilibrium point of System (12).

Employing the above Remarks, the equilibrium points L4 and L5 will be studied in Theorem 1, and all the other equilibrium points on x -axis will be investigated in Theorem 2, 3, 4.

Theorem 1: The Existence and Uniqueness of Lagrange Points L4 and L5

There is one and only one $\bar{y}_1 > 0$ such that $h(\bar{y}_1) = 0$, and only one $\bar{y}_2 < 0$ such that $h(\bar{y}_2) = 0$. That is, excluding the origin $(0,0)$ of $x - y$ plane, there are two equilibrium points on the y -axis, i.e. L4 and L5, for System (12).

(Proof): We define

$$P(y) \equiv \frac{2m}{[R^2 + y^2]^{3/2}} - n^2 \quad (19)$$

$$\text{and} \quad Q(y) \equiv c \left\{ \frac{1}{(1 + y^2)y^2} - \frac{\tan^{-1}(y)}{y^3} \right\}, \quad (20)$$

so from Eq.(17), we have $h(y) = -P(y) + Q(y)$.

We consider the case when $y > 0$ first. From Eqs. (19)-(20), we have

$$P'(y) = -6my [R^2 + y^2]^{-5/2} < 0, \quad (21)$$

and

$$Q'(y) = c \frac{-3y - 5y^3 + 3(1 + y^2)^2 \tan^{-1}(y)}{y^4(1 + y^2)^2} = c \left\{ \frac{3(1 + y^2)^2 g_1(y)}{y^4(1 + y^2)^2} \right\}, \quad (22)$$

where $g_1(y) \equiv \tan^{-1} y - \frac{5y^3+3y}{3(1+y^2)^2}$. Since $g'_1(y) = \frac{8y^4}{3(1+y^2)^3} > 0$ for $y > 0$ and $g_1(0) = 0$, we have $g_1(y) > 0$ for $y > 0$. Thus, from Eq.(22), we know $Q'(y) > 0$ for all $y > 0$. Therefore, both $P(y)$ and $Q(y)$ are monotonic functions, and $h(y) = -P(y) + Q(y)$ is a monotonically increasing function.

On the other hand, we have

$$\lim_{y \rightarrow 0} P(y) = \frac{2m}{R^3} - n^2, \quad (23)$$

and

$$\lim_{y \rightarrow \infty} P(y) = -n^2. \quad (24)$$

Moreover, using L'Hopital Rule on Eq.(20), we have

$$\begin{aligned} \lim_{y \rightarrow 0} Q(y) &= \lim_{y \rightarrow 0} \frac{c}{y^3} \left(\frac{y}{1+y^2} - \tan^{-1} y \right) \\ &= \lim_{y \rightarrow 0} \frac{-2cy^2}{3y^2(1+y^2)^2} = -\frac{2c}{3} < 0, \end{aligned} \quad (25)$$

and

$$\lim_{y \rightarrow \infty} Q(y) = \lim_{y \rightarrow \infty} \frac{c}{y^3} \left\{ \frac{y}{1+y^2} - \tan^{-1} y \right\} = 0,$$

so $-\frac{2c}{3} < Q(y) < 0$ for all $y > 0$.

Hence, from Eq. (25) and Eq. (13), we have

$$\begin{aligned} \lim_{y \rightarrow 0} h(y) &= -\lim_{y \rightarrow 0} P(y) + \lim_{y \rightarrow 0} Q(y) = -\frac{2m}{R^3} + n^2 - \frac{2c}{3} \\ &= -\frac{7m}{4R^3} + \frac{c}{R} \left| \frac{1}{(1+R^2)R} - \frac{\tan^{-1} R}{R^2} \right| - \frac{2c}{3} = -\frac{7m}{4R^3} + \left[|Q(R)| - \frac{2c}{3} \right] < 0. \end{aligned}$$

Similarly, we have $\lim_{y \rightarrow \infty} h(y) = -\lim_{y \rightarrow \infty} P(y) + \lim_{y \rightarrow \infty} Q(y) = n^2 > 0$. Because when $y > 0$, $h(y)$ is a monotonic function, there exists a unique point $\bar{y}_1 > 0$ such that $h(\bar{y}_1) = 0$.

For the case when $y < 0$, from Eq.(21)-(22), we have $P'(y) > 0, Q'(y) < 0$, so $h(y)$ is a monotonically decreasing function. We also have $\lim_{y \rightarrow 0} h(y) < 0$ and $\lim_{y \rightarrow -\infty} h(y) = n^2 > 0$. Thus, similarly, we find that there is a unique point $\bar{y}_2 < 0$ such that $h(\bar{y}_2) = 0$. Therefore, there are two equilibrium points on the line $x = 0$, i.e. y -axis. \square

In the classical restricted three-body problem, there are three collinear points, $L1, L2, L3$ and two triangular points, i.e. $L4, L5$. Theorem 1 shows the existence and uniqueness of $L4$ and $L5$ for the system we consider here.

We now investigate the existence of equilibrium points on the x -axis. For convenience, we define

$$S(x) \equiv \frac{m(x+R)}{|x+R|^3} + \frac{m(x-R)}{|x-R|^3} - n^2 x, \quad (26)$$

and therefore,

$$S(x) = \begin{cases} \frac{m}{(x+R)^2} + \frac{m}{(x-R)^2} - n^2 x, & \text{for } x > R, \\ \frac{m}{(x+R)^2} - \frac{m}{(x-R)^2} - n^2 x, & \text{for } -R < x < R, \\ -\frac{m}{(x+R)^2} - \frac{m}{(x-R)^2} - n^2 x, & \text{for } x < -R. \end{cases} \quad (27)$$

$S(x)$ includes the gravitational forces from the central binary and also the centrifugal force. From Eq.(18) and Eq.(27), we have

$$k(x) = -S(x) + c \left\{ \frac{1}{(1+x^2)x} - \frac{\tan^{-1}(x)}{x^2} \right\} = -S(x) + f_g(x), \quad (28)$$

where f_g is defined in Eq.(11). The equilibrium points on the x -axis $(x_e, 0)$ satisfy $A(x_e, 0) = k(x_e) = 0$. In addition, we define the critical mass

$$M_c \equiv \frac{51\pi m}{8[2R^3 - 3\tan^{-1} R + 3R/(1+R^2)]}, \quad (29)$$

and it is always positive as shown in Fig. 1. We also define

$$g_2(R, x) \equiv \frac{1}{(R-x)^4} - \frac{1}{(R+x)^4} \quad (30)$$

and

$$g_3(x) \equiv \frac{2}{x^4(1+x^2)^3} [9x^5 + 8x^3 + 3x - 3(1+x^2)^3 \tan^{-1} x]. \quad (31)$$

From Fig. 2, we find that there is a positive x_c such that $g_3(x_c) = 0$, and $g_3(x) > 0$ for $x \in (0, x_c)$. Because $g_3(-x) = -g_3(x)$, we also have $g_3(-x_c) = 0$ and $g_3(x) < 0$ for $x \in (-x_c, 0)$. The numerical value of $x_c \sim 1.43872$ approximately. As in Fig. 2, we find that when $x_c < x < R$, there is a lower bound g_{3c} for $g_3(x)$ such that $g_{3c} < g_3(x) < 0$. The numerical value of $g_{3c} \sim -0.057$ approximately. Finally, we define

$$g_4(R) \equiv \frac{1}{(R-x_c)^4} - \frac{1}{(R+x_c)^4} + \frac{17g_{3c}}{8[2R^3 - 3\tan^{-1} R + 3R/(1+R^2)]}. \quad (32)$$

As shown in Fig. 3, $g_4(R) > 0$ for any R . The above definitions of M_c , $g_2(R, x)$, $g_3(x)$, x_c , g_{3c} , $g_4(R)$, and their properties will be employed in below three theorems.

In the following Theorem 2, the results show the existence of three equilibrium points, i.e. Lagrange Point 1, 2, and 3 (L1-L3). In Theorem 3, we show that when the total mass

of the galaxy $M_g > M_c$, two more equilibrium points, i.e. Jiang-Yeh Point 1 (JY1) and Jiang-Yeh Point 2 (JY2), exist. In Theorem 4, the results show that when the total mass of the galaxy $M_g < M_c$, neither JY1 nor JY2 exist. Therefore, Jiang-Yeh Points exist if and only if the total galactic mass is larger than the critical mass.

For convenience, in the following proofs of Theorem 2, 3, and 4, we denote R^+ to represent that x tends to R from the right hand side and R^- to represent that x tends to R from the left hand side.

Theorem 2: The Existence of Lagrange Points L1, L2, and L3

- (i) There is an $x_1 > R$ and an $x_2 < -R$ such that $k(x_1) = 0$ and $k(x_2) = 0$. That is, on the x -axis, there is an equilibrium point in the region (R, ∞) , and there is an equilibrium point in the region $(-\infty, -R)$
- (ii) The origin $(0,0)$ is an equilibrium point, i.e. $k(0) = 0$.

(Proof):

- (i) When $x > R$, from Eqs. (27)-(28),

$$k(x) = -S(x) + f_g(x) = -\frac{m}{(x+R)^2} - \frac{m}{(x-R)^2} + n^2x + c \left\{ \frac{1}{(1+x^2)x} - \frac{\tan^{-1}(x)}{x^2} \right\}.$$

Thus, we have $\lim_{x \rightarrow R^+} k(x) = \lim_{x \rightarrow R^+} -S(x) + f_g(x) = -\infty$ and $\lim_{x \rightarrow \infty} k(x) = \lim_{x \rightarrow \infty} -S(x) + f_g(x) = \infty$. Therefore, there is a point $x_1 > R$ such that $k(x_1) = 0$.

When $x < -R$, using the similar method, we have that there is a point $x_2 < -R$ such that $k(x_2) = 0$.

- (ii) When $-R < x < R$, from Eq. (27), we have

$$S(x) = \frac{m}{(x+R)^2} - \frac{m}{(x-R)^2} - n^2x. \quad (33)$$

Thus, $S(0) = 0$. Moreover, from Eq.(28), we employ L'Hopital Rule and obtain,

$$\lim_{x \rightarrow 0} f_g(x) = \lim_{x \rightarrow 0} c \left\{ \frac{x - (1+x^2)\tan^{-1}x}{(1+x^2)x^2} \right\} = \lim_{x \rightarrow 0} \frac{-c\tan^{-1}x}{1+2x^2} = 0.$$

Therefore,

$$k(0) = S(0) + \lim_{x \rightarrow 0} f_g(x) = 0$$

and the origin $(0,0)$ is an equilibrium point. \square

Theorem 3: The Existence of Jiang-Yeh Points JY1 and JY2

If $M_g > M_c$, where M_c is the critical mass defined in Eq. (29), then there is an $x_4 \in (0, R)$

such that $k(x_4) = 0$ and an $x_5 \in (-R, 0)$ such that $k(x_5) = 0$.

(Proof):

When $-R < x < R$, from Eq.(11) and Eq.(33), we have

$$S'(x) = -\frac{2m}{(x+R)^3} + \frac{2m}{(x-R)^3} - n^2 \quad (34)$$

$$\text{and } f'_g(x) = 2c \left\{ \frac{-2x^3 - x + (1+x^2)^2 \tan^{-1} x}{x^3(1+x^2)^2} \right\}. \quad (35)$$

Thus,

$$S'(0) = -\frac{4m}{R^3} - n^2 \quad (36)$$

and

$$\begin{aligned} \lim_{x \rightarrow 0} f'_g(x) &= \lim_{x \rightarrow 0} 2c \left\{ \frac{-2x^3 - x + (1+x^2)^2 \tan^{-1} x}{x^3(1+x^2)^2} \right\} \\ &= 2c \lim_{x \rightarrow 0} \frac{-5x^2 + 4x(1+x^2) \tan^{-1} x}{x^2(1+x^2)(3+7x^2)} \\ &= 2c \lim_{x \rightarrow 0} \frac{-6x + 4(1+3x^2) \tan^{-1} x}{6x + 40x^3 + 42x^5} \\ &= 2c \lim_{x \rightarrow 0} \frac{-6 + 24x \tan^{-1} x + 4 \frac{1+3x^2}{1+x^2}}{6 + 120x^2 + 210x^4} \\ &= -\frac{2c}{3} \end{aligned} \quad (37)$$

From Eq.(13), Eq.(37) and Eq.(29), we have

$$\begin{aligned} k'(0) &= -S'(0) + f'_g(0) \\ &= \frac{4m}{R^3} + n^2 - \frac{2c}{3} \\ &= \frac{17m}{4R^3} + \frac{c}{R} \left| \frac{1}{(1+R^2)R} - \frac{\tan^{-1} R}{R^2} \right| - \frac{2c}{3} \\ &= \frac{1}{R^3} \left\{ \frac{17m}{4} + \frac{2M_g}{\pi} \left[-\frac{2R^3}{3} + \tan^{-1} R - \frac{R}{(1+R^2)} \right] \right\} \\ &= \frac{1}{R^3} \left\{ \frac{17m}{4} + \frac{2M_g}{\pi} \left(-\frac{17\pi m}{8M_c} \right) \right\} \\ &= \frac{17m}{4R^3 M_c} (M_c - M_g), \end{aligned} \quad (38)$$

where M_c is defined in Eq. (29). Due to the condition $M_g > M_c$, we obtain $k'(0) < 0$.

We first consider the region with $0 < x < R$. From Eq.(11) and Eq. (33), we have $\lim_{x \rightarrow R^-} S(x) = -\infty$ and $-\infty < f_g(R) < 0$. Thus,

$$\lim_{x \rightarrow R^-} k(x) = \lim_{x \rightarrow R^-} -S(x) + f_g(x) = \infty.$$

Because $k(0) = 0$, $k'(0) < 0$, and $\lim_{x \rightarrow R^-} k(x) = \infty$, as x increases from zero, $k(x)$ becomes negative first and needs to be positive when x approaches to R . Therefore, there is a point $0 < x_4 < R$ such that $k(x_4) = 0$.

Similarly, for the region with $-R < x < 0$, we have $\lim_{x \rightarrow -R^+} k(x) = -\infty$, $k'(0) < 0$, and $k(0) = 0$. As x increases from $-R$, $k(x)$ is negative first and needs to be positive when x is very close to zero due to that $k(0) = 0$ and $k'(0) < 0$. Therefore, there is a point $x_5 \in (-R, 0)$ such that $k(x_5) = 0$. \square

Theorem 4: The Nonexistence of Jiang-Yeh Points JY1 and JY2

When $M_g < M_c$, there is no any $x \in (-R, 0)$ or $x \in (0, R)$ such that $k(x) = 0$.

(Proof): Because $M_g < M_c$, from Eq. (38), we have

$$k'(0) = \frac{17m}{4R^3 M_c} (M_c - M_g) > 0.$$

Since we will need to calculate $k''(x)$ later and $k''(x) = -S''(x) + f_g''(x)$, we calculate $S''(x)$ and $f_g''(x)$ here. When $-R < x < R$, from Eq. (34)-(35), we have

$$S''(x) = \frac{6m}{(x+R)^4} - \frac{6m}{(x-R)^4} = -6mg_2(R, x).$$

As we show in Appendix A, $S''(x) > 0$ for $x \in (-R, 0)$ and $S''(x) < 0$ for $x \in (0, R)$.

If there is an x such that $x_c < x < R$ (for the case $R > x_c$), we have $-S''(x) > 6mg_2(R, x_c)$ as shown in Appendix B.

Moreover,

$$f_g''(x) = 2c \left\{ \frac{9x^5 + 8x^3 + 3x - 3(1+x^2)^3 \tan^{-1} x}{x^4(1+x^2)^3} \right\} = cg_3(x).$$

where $g_3(x)$ is defined in Eq.(31). Thus, the behavior of $f_g''(x)$ is completely determined by the properties of $g_3(x)$. For example, $f_g''(x_c) = cg_3(x_c) = 0$. Moreover, for $x > 0$, we have $g_3(x) > g_{3c}$, where g_{3c} is the lower bound of $g_3(x)$. Thus, $f_g''(x) = cg_3(x) > cg_{3c}$ for any $x \in (0, R)$.

Case 1: If $R < x_c$, then $g_3(x) > 0$ for any $x \in (0, R)$ and $g_3(x) < 0$ for $x \in (-R, 0)$. We thus have $f_g''(x) > 0$ for any $x \in (0, R)$ and $f_g''(x) < 0$ for $x \in (-R, 0)$.

We first consider the $0 < x < R$ region. Since $k'(0) > 0$ and $k''(x) = -S''(x) + f_g''(x) > 0$ for any $x \in (0, R)$, we have $k'(x) > 0$. Because $k(0) = 0$ and $k'(x) > 0$ for $0 < x < R$, there is no $x \in (0, R)$ such that $k(x) = 0$.

Similarly, we have $k(0) = 0$ and $k'(x) > 0$ for $-R < x < 0$, so there is no any $x \in (-R, 0)$ such that $k(x) = 0$.

Case 2: If $R > x_c$, it will be more complicated as the x we consider can be either larger or smaller than x_c , such that $g_3(x)$ and $f_g''(x)$ can be negative or positive in the region $x \in (0, R)$.

(1) When $x < x_c$, we have $0 < x < x_c < R$ here. Thus, $S''(x) < 0$, $g_3(x) > 0$, and $f_g''(x) > 0$, so $k''(x) = -S''(x) + f_g''(x) > 0$.

(2) When $x = x_c$, we have $g_3(x) = 0$ and thus $f_g''(x) = 0$. Due to that $S''(x) < 0$, $k''(x) = -S''(x) + f_g''(x) > 0$.

(3) When $x > x_c$, we have $-S''(x) > 6mg_2(R, x_c)$, and $f_g''(x) = cg_3(x) > cg_{3c}$. Moreover, due to that $g_{3c} < 0$ and $M_g < M_c$, we have $M_g g_{3c} > M_c g_{3c}$. Therefore, as defined before $c = 2M_g/\pi$ and from the definition of M_c in Eq. (29), we obtain

$$\begin{aligned} k''(x) &= -S''(x) + f_g''(x) > 6mg_2(R, x_c) + \frac{2}{\pi}M_g g_{3c}. \\ &> 6mg_2(R, x_c) + \frac{2}{\pi}M_c g_{3c} \\ &= 6m \left\{ \frac{1}{(R - x_c)^4} - \frac{1}{(R + x_c)^4} + \frac{17g_{3c}}{8[2R^3 - 3\tan^{-1}R + 3R/(1 + R^2)]} \right\} \\ &= 6mg_4(R). \end{aligned}$$

Although $g_2(R, x_c) > 0$ and $g_{3c} < 0$, since $g_4(R) > 0$ as shown in Fig. 3, we obtain $k''(x) > 0$. From (1), (2), and (3), we know that $k''(x) > 0$ for any $x \in (0, R)$, no matter $x > x_c$ or not.

Therefore, due to that $k'(0) > 0$ and $k''(x) > 0$ for any $x \in (0, R)$, we have $k'(x) > 0$. Since $k(0) = 0$ and $k'(x) > 0$, there is no $x \in (0, R)$ such that $k(x) = 0$.

For $-R < x < 0$, by a similar procedure, it can be shown that there is no $x \in (-R, 0)$ such that $k(x) = 0$ under the same condition. This concludes our proof of non-existence of JY1 and JY2. \square

4. The Bifurcations and Zero-Velocity Curves

In order to demonstrate the analytic results proved above, we determine the locations of equilibrium points numerically by solving $k(x) = 0$, and $h(y) = 0$, and plot in Fig. 4-5. The locations of the equilibrium points on the x -axis with $m = 1$ for different values of M_g are in Fig.4 (Panel (a) is for $R = 0.25$ and Panel (b) is for $R = 0.5$) and Fig.5 (Panel (a) is for $R = 1$ and Panel (b) is for $R = 2$).

The values of the critical mass M_c depend on m and R . For Fig.4(a) with $m = 1$ and $R = 0.25$, we find that $M_c = 9118.55$. Due to that M_c is very huge, the value of M_g cannot be larger than M_c and there are always three equilibrium points, i.e. Lagrange Points, on the $x - axis$ for whole range of M_g in that plot. For Fig.4(b) with $m = 1$ and $R = 0.5$, we find that $M_c = 339.12$. In this panel, the plot shows that there are three equilibrium points, i.e. Lagrange Points L1, L2, L3, when $M_g < M_c$ and bifurcate into five equilibrium points, i.e. Lagrange Points, L1, L2, L3, and Jiang-Yeh Points, JY1, JY2, when $M_g > M_c$. As expected, the location of JY1 is in $(0, R)$ and the location of JY2 is in $(-R, 0)$ for this case with $R = 0.5$.

For Fig.5(a) with $m = 1$ and $R = 1$, we find that $M_c = 17.51$. Similarly, three equilibrium points, L1, L2, L3, bifurcate into five equilibrium points, L1, L2, L3, JY1, JY2, when M_g passes through the value of M_c . Finally, in Fig. 5(b) with $m = 1$ and $R = 2$, we find that the critical mass $M_c = 1.44$. Given that this M_c is small, there are three equilibrium points on the very left part, and five equilibrium points for the most part of this plot.

In Fig. 6, the zero-velocity curves, which are obtained through Eq.(14), of the case with $m = 1$ and $R = 1$ are presented. Fig. 6(a) is for $M_g = 10$, Fig. 6(b) is for $M_g = 20$, Fig. 6(c) is for $M_g = 30$, and Fig. 6(d) is for $M_g = 100$. The + signs are the locations for Lagrange Points, and the squares indicate the Jiang-Yeh Points. These points are numerically determined by solving $k(x) = 0$ and $h(y) = 0$. Fig. 6 shows that they are completely consistent with the locations of equilibrium points implied by zero-velocity curves. Due to that the critical mass $M_c = 17.51$, apparently, only Lagrange Points exist in Fig. 6(a), but both Lagrange Points (L1-L5) and Jiang-Yeh Points (JY1-JY2) exist in Fig. 6(b)-(d). The locations and the Jacobi integral C_J of all equilibrium points shown in Fig. 6 are summarized in Table 1.

Table 1. The Locations and C_J of Equilibrium Points

$M_g = 10$							
	L1		L2	L3	L4	L5	
(x_e, y_e)	(0,0)		(1.70,0)	(-1.70,0)	(0,1.15)	(0,-1.15)	
C_J	16.73		17.35		14.82		
$M_g = 20$							
	L1	L2	L3	L4	L5	JY1	JY2
(x_e, y_e)	(0,0)	(1.57,0)	(-1.57,0)	(0,1.09)	(0,-1.09)	(0.18,0)	(-0.18,0)
C_J	29.46	30.14		26.67		29.45	
$M_g = 30$							
	L1	L2	L3	L4	L5	JY1	JY2
(x_e, y_e)	(0,0)	(1.50,0)	(-1.50,0)	(0,1.06)	(0,-1.06)	(0.36,0)	(-0.36,0)
C_J	42.19	42.65		38.50		42.0	
$M_g = 100$							
	L1	L2	L3	L4	L5	JY1	JY2
(x_e, y_e)	(0,0)	(1.34,0)	(-1.34,0)	(0,1.02)	(0,-1.02)	(0.62,0)	(-0.62,0)
C_J	131.32	128.15		121.24		127.55	

5. The Stability of Equilibrium Points

The equations of the considered system can be written as

$$\left\{ \begin{array}{l} \frac{dx}{dt} = u, \\ \frac{dy}{dt} = v, \\ \frac{du}{dt} = 2nv + A(x, y), \\ \frac{dv}{dt} = -2nu + B(x, y), \end{array} \right. \quad (39)$$

where $A(x, y)$, $B(x, y)$ are defined in Eqs.(15)-(16).

To study the stability of equilibrium points, we need to know the properties of eigenvalues of equilibrium points. The characteristic equation of the eigen-value λ is

$$\lambda^4 + (4n^2 - A_x - B_y)\lambda^2 + 2n(A_y - B_x)\lambda + A_x B_y - B_x A_y = 0, \quad (40)$$

where $A_x \equiv \partial A(x, y)/\partial x$, $A_y \equiv \partial A(x, y)/\partial y$, $B_x \equiv \partial B(x, y)/\partial x$, and $B_y \equiv \partial B(x, y)/\partial y$. Thus,

$$\begin{aligned} A_x = & n^2 - \frac{m}{r_1^3} - \frac{m}{r_2^3} + \frac{3m(x+R)^2}{r_1^5} + \frac{3m(x-R)^2}{r_2^5} + \frac{c}{r} \left\{ \frac{1}{(1+r^2)r} - \frac{\tan^{-1}(r)}{r^2} \right\} \\ & + \frac{cx}{r} \left\{ \frac{-5r^3 - 3r + 3(1+r^2)^2 \tan^{-1} r}{(1+r^2)^2 r^3} \right\}, \end{aligned} \quad (41)$$

$$A_y = \frac{3m(x+R)y}{r_1^5} + \frac{3m(x-R)y}{r_2^5} + \frac{cxy(-5r^3 - 3r + 3(1+r^2)^2 \tan^{-1} r)}{(1+r^2)^2 r^5}, \quad (42)$$

$$B_x = \frac{3my(x+R)}{r_1^5} + \frac{3my(x-R)}{r_2^5} + \frac{cxy(-5r^3 - 3r + 3(1+r^2)^2 \tan^{-1} r)}{(1+r^2)^2 r^5}, \quad (43)$$

$$B_y = n^2 - \frac{m}{r_1^3} - \frac{m}{r_2^3} + \frac{3my^2}{r_1^5} + \frac{3my^2}{r_2^5} + \frac{c}{r} \left\{ \frac{1}{(1+r^2)r} - \frac{\tan^{-1}(r)}{r^2} \right\} + \frac{cy^2(-5r^3 - 3r + 3(1+r^2)^2 \tan^{-1} r)}{(1+r^2)^2 r^5}. \quad (44)$$

From Eq.(42) and Eq.(43), for any x_e we have $A_y(x_e, 0) = B_x(x_e, 0) = 0$, and for any y_e we have $A_y(0, y_e) = B_x(0, y_e) = 0$.

In order to do further investigation, some parameters need to be specified and we set $m = 1$ and $R = 1$ for all the results in this section. Thus, from Eq.(11), Eq.(13), and Eq.(29) we have

$$n^2 = \frac{1}{4} + \frac{2M_g}{\pi} \left(\frac{\pi}{4} - \frac{1}{2} \right),$$

and

$$M_c = \frac{51\pi}{28 - 6\pi} \sim 17.5.$$

At first, we consider the equilibrium point L2 or JY1, (x_e, y_e) , which satisfies $k(x_e) = 0$ with $x_e > 0$ and $y_e = 0$. Because $A_y(x_e, 0) = 0$ and $B_x(x_e, 0) = 0$, Eq.(40) becomes

$$\lambda^4 + (4n^2 - A_x - B_y)\lambda^2 + A_x B_y = 0. \quad (45)$$

For convenience, we define $\Omega = A_x B_y$ and $\Pi \equiv A_x + B_y - 4n^2$. Therefore, we have

$$\lambda_+^2 = \frac{\Pi + \sqrt{\Pi^2 - 4\Omega}}{2} \quad \text{and} \quad \lambda_-^2 = \frac{\Pi - \sqrt{\Pi^2 - 4\Omega}}{2}. \quad (46)$$

Moreover, $A_x(x_e, 0)$ and $B_y(x_e, 0)$ can be expressed as:

$$\begin{aligned} A_x(x_e, 0) &= 3n^2 - \frac{2}{x_e} \left(\frac{1}{|x_e + 1|^3} - \frac{1}{|x_e - 1|^3} \right) - \frac{4M_g}{\pi(1 + x_e^2)^2} \\ &= \frac{3}{4} + \frac{6M_g}{\pi} \left(\frac{\pi}{4} - \frac{1}{2} \right) - \frac{2}{x_e} \left(\frac{1}{|x_e + 1|^3} - \frac{1}{|x_e - 1|^3} \right) - \frac{4M_g}{\pi(1 + x_e^2)^2}, \end{aligned} \quad (47)$$

$$B_y(x_e, 0) = \frac{1}{x_e} \left(\frac{1}{|x_e + 1|^3} - \frac{1}{|x_e - 1|^3} \right) < 0. \quad (48)$$

For the equilibrium point L2, $x_e > R = 1$, so $(1 + x_e^2)^2 > 4$. Thus,

$$- \frac{4M_g}{\pi(1 + x_e^2)^2} > - \frac{M_g}{\pi}. \quad (49)$$

Because $x_e > 1$ leads to

$$\frac{3}{4} - \frac{2}{x_e} \left(\frac{1}{|x_e + 1|^3} - \frac{1}{|x_e - 1|^3} \right) > 0,$$

with Eq.(47) and Eq.(49), we obtain

$$A_x(x_e, 0) > \frac{6M_g}{\pi} \left(\frac{\pi}{4} - \frac{1}{2} \right) - \frac{4M_g}{\pi(1+x_e^2)^2} > \frac{M_g}{\pi} \left(\frac{3\pi}{2} - 4 \right) > 0.$$

Since $A_x(x_e, 0) > 0$ and $B_y(x_e, 0) < 0$, we have $\Omega = A_x(x_e, 0)B_y(x_e, 0) < 0$. Thus, $\Pi^2 - 4\Omega > 0$, and we have $\lambda_+^2 > 0$ and $\lambda_-^2 < 0$. As in Szebehely (1967), this result indicates that it is an unstable equilibrium point.

For the equilibrium point JY1 (which we assume it exists with $M_g > M_c$), it has $0 < x_e < 1$ and $y_e = 0$. For a given M_g , we numerically search the location of JY1, and then obtain the corresponding $A_x(x_e, 0)$. The numerical value of $A_x(x_e, 0)$ as a function of M_g is shown in Fig. 7(a). It shows that $A_x(x_e, 0) > 0$ for the considered M_g . From Eq.(48), we have $B_y(x_e, 0) < 0$ here and so $\Omega = A_x B_y < 0$. Thus, $\Pi^2 - 4\Omega > 0$, we have $\lambda_+^2 > 0$ and $\lambda_-^2 < 0$. Therefore, JY1 is also an unstable equilibrium point. Because our system is symmetric with respect to the y -axis, the above results imply that the equilibrium point L3 and JY2 are unstable.

Secondly, we study the equilibrium point L4, which can be written as $(0, y_e)$ with $y_e > 0$. As mentioned previously, we have $A_y(0, y_e) = B_x(0, y_e) = 0$. Thus, Eq.(45) and Eq.(46) are also valid here. We find that

$$A_x(0, y_e) = \frac{6}{(1+y_e^2)^{3/2}} > 0, \quad (50)$$

but cannot determine the sign of $B_y(0, y_e)$ analytically. Thus, for each given M_g , the location of L4, $(0, y_e)$, and then the corresponding value of $\Pi^2 - 4\Omega$ is determined numerically. For $M_g < 100$, we find that $\Pi^2 - 4\Omega < 0$ as shown in Fig. 7(b). Thus, both λ_+^2 and λ_-^2 are complex numbers. This leads to that both λ_+ and λ_- have a root which contains positive real part, so that L4 is unstable. As our system is symmetric with respect to the x -axis, the equilibrium point L5 is therefore unstable.

Thirdly, we study the equilibrium point L1, $(0,0)$, here. As A_x, A_y, B_x, B_y contain terms that both denominator and numerator become zero at $(x, y) = (0, 0)$, we consider the limit that r approaches to zero and employ L'Hopital Rule for the following results (see Appendix C for the details). We obtain $A_y(0, 0) = 0$ and $B_x(0, 0) = 0$, so Eq.(45) and Eq.(46) are also valid for L1 here. In addition, we have $B_y(0, 0) < 0$, and

$$A_x(0, 0) = \frac{17}{4M_c}(M_c - M_g). \quad (51)$$

When $M_g < M_c$, $A_x(0,0) > 0$ and thus $\Omega < 0$. Therefore, $\Pi^2 - 4\Omega > 0$, and we have $\lambda_+^2 > 0$, $\lambda_-^2 < 0$. This leads to an unstable point. When $M_g > M_c$, $A_x(0,0) < 0$ and thus $\Omega > 0$. The sign of $\Pi^2 - 4\Omega$ cannot be determined analytically. It is shown in Fig. 7(c) numerically that $\Pi^2 - 4\Omega > 0$. Further, we can show that (see Appendix C)

$$\Pi = \frac{3}{2} - \frac{2}{\pi} M_g \left(\frac{\pi}{2} + \frac{1}{3} \right). \quad (52)$$

Since Π has a simple linear dependence on M_g , it is trivial that $\Pi < 0$ for the considered value of M_g here. This leads to that both λ_+^2 and λ_-^2 are real and negative. Thus, both λ_+ and λ_- are pure imaginary numbers. Therefore, L1 is a center for this case.

In this section, we have shown that (1) when $M_g < M_c$, there are five equilibrium points in total, i.e. L1, L2, L3, L4, L5, and all of them are unstable; (2) when $M_g > M_c$, there are seven equilibrium points in total, and among these, L2, L3, L4, L5, JY1, JY2 are unstable, but L1 is neutrally stable.

6. The Summary

We have studied the equilibrium points of a galactic system with a supermassive binary black hole. Focusing on the case with an equal mass binary black hole, the conditions of existence of equilibrium points, including Lagrange Points and Jiang-Yeh Points, are investigated. A necessary and sufficient condition for the existence of Jiang-Yeh Points is found. That is, Jiang-Yeh Points exist if and only if the total galactic mass is larger than the critical mass. The further stability analysis shows that Jiang-Yeh Points are unstable. Thus, many stars might be ejected from the region near Jiang-Yeh Points after a supermassive binary black hole come to near the core of a galaxy during merging events. Therefore, the unstable Jiang-Yeh Points could lead to a mechanism to form galactic cores, as those observed in Lauer et al. (2007). Although N-body simulations are needed to confirm this possible explanation about the core formation of galaxies, we conclude that our model and the results are fundamentally important for the study of galactic structures.

Acknowledgment

We thank the referee for very good suggestions which greatly improved this paper. We are grateful to the National Center for High-performance Computing for computer time and facilities. This work is supported in part by the National Science Council, Taiwan, under Ing-Guey Jiang's Grants NSC 100-2112-M-007-003-MY3 and Li-Chin Yeh's Grants NSC 100-2115-M-134-004.

REFERENCES

- Chermnykh, S. V., 1987, Vest. Leningrad Univ. 2, 10
- Ji, J., Li, G., Liu, L., 2002, ApJ, 572, 1041
- Jiang, I.-G., Ip, W.-H., 2001, A&A, 367, 943
- Jiang, I.-G., Ip, W.-H., Yeh, L.-C., 2003, ApJ, 582, 449
- Jiang, I.-G., Yeh, L.-C., 2003, Int. J. Bifurcation and Chaos, 13, 617
- Jiang, I.-G., Yeh, L.-C., 2004a, AJ, 128, 923
- Jiang, I.-G., Yeh, L.-C., 2004b, Int. J. Bifurcation and Chaos, 14, 3153
- Jiang, I.-G., Yeh, L.-C., 2004c, MNRAS, 355, L29
- Jiang, I.-G., Yeh, L.-C., 2006, Astrophysics and Space Science, 305, 341
- Jiang, I.-G., Yeh, L.-C., 2007, ApJ, 656, 534
- Jiang, I.-G., Yeh, L.-C., 2009, AJ, 137, 4169
- Jiang, I.-G., Yeh, L.-C., 2011, MNRAS, 415, 2859
- Jiang, I.-G., Yeh, L.-C., Hung, W.-L., Yang, M.-S., 2006, MNRAS, 370, 1379
- Jiang, I.-G., Yeh, L.-C., Chang, Y.-C., Hung, W.-L., 2007, AJ, 134, 2061
- Jiang, I.-G., Yeh, L.-C., Chang, Y.-C., Hung, W.-L., 2009, AJ, 137, 329
- Jiang, I.-G., Yeh, L.-C., Chang, Y.-C., Hung, W.-L., 2010, ApJS, 186, 48
- Jiang, I.-G. et al., 2013, AJ, 145, 68
- Kandrup, H. E., Sideris, I. V., Terzic, B. Bohn, C. L., 2003, ApJ, 597, 111
- Kushvah, B. S., 2008a, Astrophysics and Space Science, 315, 231
- Kushvah, B. S., 2008b, Astrophysics and Space Science, 318, 41
- Kushvah, B. S., 2009, Astrophysics and Space Science, 323, 57
- Kushvah, B. S., 2011a, Astrophysics and Space Science, 332, 99
- Kushvah, B. S., 2011b, Astrophysics and Space Science, 333, 49

- Lauer, T. R. et al., 1995, *AJ*, 110, 2622
- Lauer, T. R. et al., 2007, *ApJ*, 664, 226
- Murray, C. D., Dermott, S. F., 1999, *Solar System Dynamics* (Cambridge: Cambridge University Press)
- Papadakis, K. E., 2004, *A&A*, 425, 1133
- Papadakis, K. E., 2005a, *Astrophysics and Space Science*, 299, 67
- Papadakis, K. E., 2005b, *Astrophysics and Space Science*, 299, 129
- Szebehely, V., 1967, *Theory of Orbits: The Restricted Problem of Three Bodies* (London: Academic Press, Inc.)
- Yeh, L.-C., Chen, Y.-C., Jiang, I.-G., 2012, *Int. J. Bifurcation and Chaos*, 22, 1230040
- Yeh, L.-C., Jiang, I.-G., 2006, *Astrophysics and Space Science*, 306, 189

Appendix A

Lemma 1: $S''(x) > 0$ for $-R < x < 0$ and $S''(x) < 0$ for $0 < x < R$

(Proof):

If $-R < x < 0$, then $|x - R| > |x + R|$ and $(x - R)^4 > (x + R)^4$. Thus, $S''(x) = 6m \left\{ \frac{1}{(x+R)^4} - \frac{1}{(x-R)^4} \right\} > 0$. On the other hand, if $0 < x < R$, then $|x + R| > |x - R|$ and $(x + R)^4 > (x - R)^4$. Therefore, $S''(x) = 6m \left\{ \frac{1}{(x+R)^4} - \frac{1}{(x-R)^4} \right\} < 0$. \square

Appendix B

Lemma 2: If $x_c < x < R$, then $-S''(x) > 6mg_2(R, x_c)$.

(Proof):

If $x_c < x < R$, then $|x_c - R| > |x - R|$ and $|x + R| > |x_c + R|$. Moreover, we have $(x_c - R)^4 > (x - R)^4$ and $(x + R)^4 > (x_c + R)^4$. Thus, From Eq. (30),

$$S''(x) = 6m \left\{ \frac{1}{(x+R)^4} - \frac{1}{(x-R)^4} \right\} < 6m \left\{ \frac{1}{(x_c+R)^4} - \frac{1}{(x_c-R)^4} \right\} = -6mg_2(R, x_c),$$

so $-S''(x) > 6mg_2(R, x_c)$. \square

Appendix C

The calculations of $A_x(0, 0)$, $A_y(0, 0)$, $B_x(0, 0)$, $B_y(0, 0)$ are presented here. The results here were used in the section of stability analysis.

For $A_x(0, 0)$, we first consider the summation of 2nd to 5th terms. Because we set $m = 1$ and $R = 1$ for the results in the section of stability analysis, $r_1 = r_2 = 1$ and thus

$$\lim_{r \rightarrow 0} -\frac{m}{r_1^3} - \frac{m}{r_2^3} + \frac{3m(x+R)^2}{r_1^5} + \frac{3m(x-R)^2}{r_2^5} = 4. \quad (53)$$

We then apply the L'Hopital Rule on the 6th term of Eq. (41) as

$$\begin{aligned} & \lim_{r \rightarrow 0} \frac{c}{r} \left\{ \frac{1}{(1+r^2)r} - \frac{\tan^{-1}(r)}{r^2} \right\} \\ &= \lim_{r \rightarrow 0} \frac{c[r - (1+r^2)\tan^{-1}r]}{(1+r^2)r^3} \\ &= \lim_{r \rightarrow 0} \frac{c[1 - 1 - 2r\tan^{-1}r]}{5r^4 + 3r^2} \\ &= \lim_{r \rightarrow 0} \frac{-2c\tan^{-1}r}{5r^3 + 3r} \\ &= \lim_{r \rightarrow 0} \frac{-2c\frac{1}{1+r^2}}{15r^2 + 3} \end{aligned}$$

$$= -\frac{2c}{3} \quad (54)$$

Similarly, the 7th term becomes

$$\begin{aligned} & \lim_{r \rightarrow 0} \frac{cx}{r} \left\{ \frac{-5r^3 - 3r + 3(1+r^2)^2 \tan^{-1} r}{(1+r^2)^2 r^3} \right\} \\ &= \lim_{r \rightarrow 0} \frac{cx}{r} \lim_{r \rightarrow 0} \left\{ \frac{-5r^3 - 3r + 3(1+r^2)^2 \tan^{-1} r}{(1+r^2)^2 r^3} \right\} \\ &= c \lim_{r \rightarrow 0} \frac{-12r^2 + 12r(1+r^2) \tan^{-1} r}{3r^2 + 10r^4 + 7r^6} \\ &= c \lim_{r \rightarrow 0} \frac{-24r + 12r + 12(1+3r^2) \tan^{-1} r}{6r + 40r^3 + 42r^5} \\ &= c \lim_{r \rightarrow 0} \frac{-12 + 12 \frac{1+3r^2}{1+r^2} + 72r \tan^{-1} r}{6 + 120r^2 + 210r^4} \\ &= 0. \end{aligned} \quad (55)$$

From the above results and $c = 2M_g/\pi$,

$$\begin{aligned} A_x(0,0) &= n^2 + 4 - \frac{2c}{3} \\ &= n^2 + 4 - \frac{4}{3\pi} M_g \\ &= \frac{17}{4} + \frac{2M_g}{\pi} \left(\frac{\pi}{4} - \frac{1}{2} \right) - \frac{4M_g}{3\pi} \\ &= \frac{17}{4} + \left(\frac{1}{2} - \frac{7}{3\pi} \right) M_g \\ &= \frac{17}{4M_c} (M_c - M_g). \end{aligned} \quad (56)$$

Through the similar process, we can easily show that $A_y(0,0) = 0$, $B_x(0,0) = 0$ and also obtain that

$$\begin{aligned} B_y(0,0) &= n^2 - 2 - \frac{2c}{3} \\ &= n^2 - 2 - \frac{4M_g}{3\pi} \\ &= -\frac{7}{4} - \frac{4}{3\pi} M_g + \frac{2M_g}{\pi} \left(\frac{\pi}{4} - \frac{1}{2} \right) \\ &= -\frac{7}{4} + \frac{2M_g}{\pi} \left(\frac{\pi}{4} - \frac{7}{6} \right) \\ &< 0. \end{aligned} \quad (57)$$

The corresponding Π is defined as

$$\begin{aligned}\Pi &\equiv A_x(0,0) + B_y(0,0) - 4n^2 \\ &= -2n^2 + 2 - \frac{8}{3\pi}M_g \\ &= \frac{3}{2} - \frac{2}{\pi}M_g \left(\frac{\pi}{2} + \frac{1}{3} \right),\end{aligned}\tag{58}$$

which is a linear function of M_g .

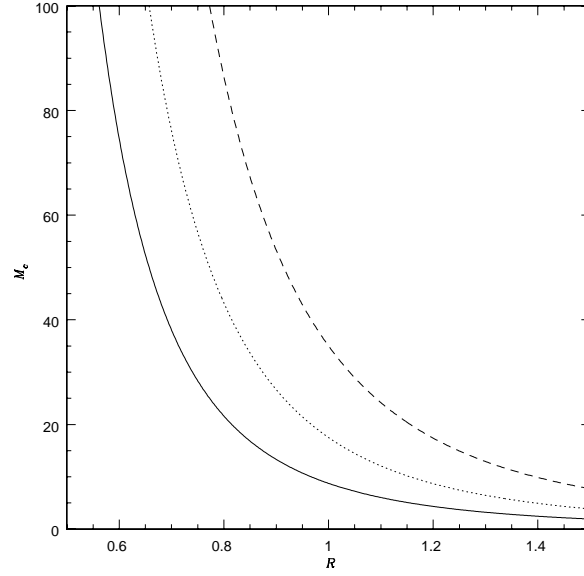


Fig. 1.— The behavior of M_c as a function of R . The solid curve is for $m = 0.5$, the dotted curve is for $m = 1$, and the dashed curve is for $m = 2$.

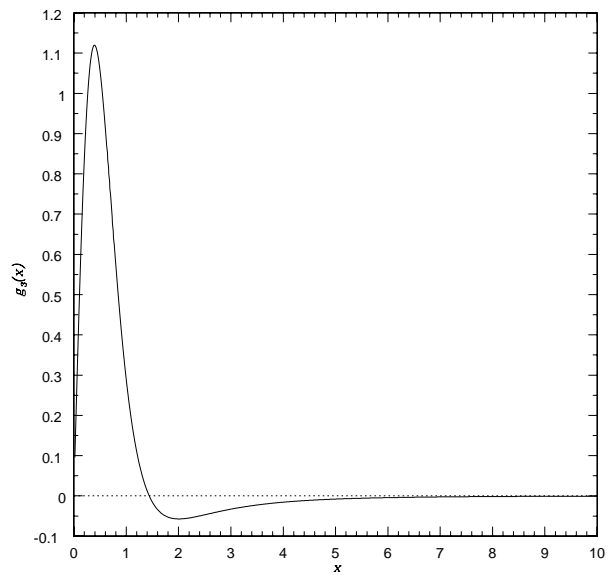


Fig. 2.— The behavior of the function $g_3(x)$.

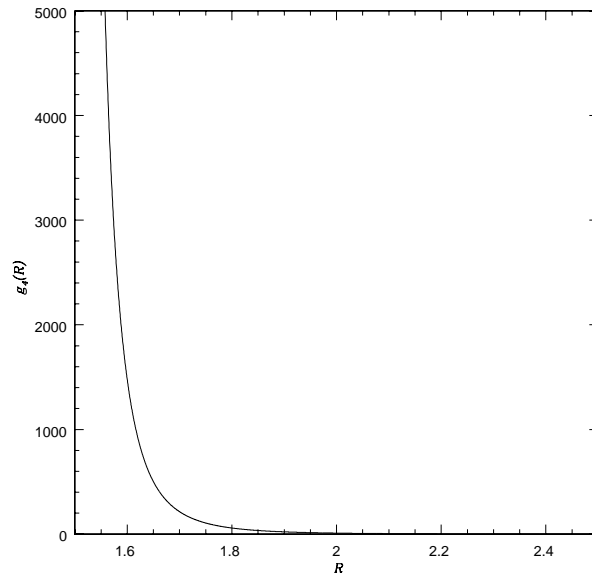


Fig. 3.— The behavior of the function $g_4(R)$.

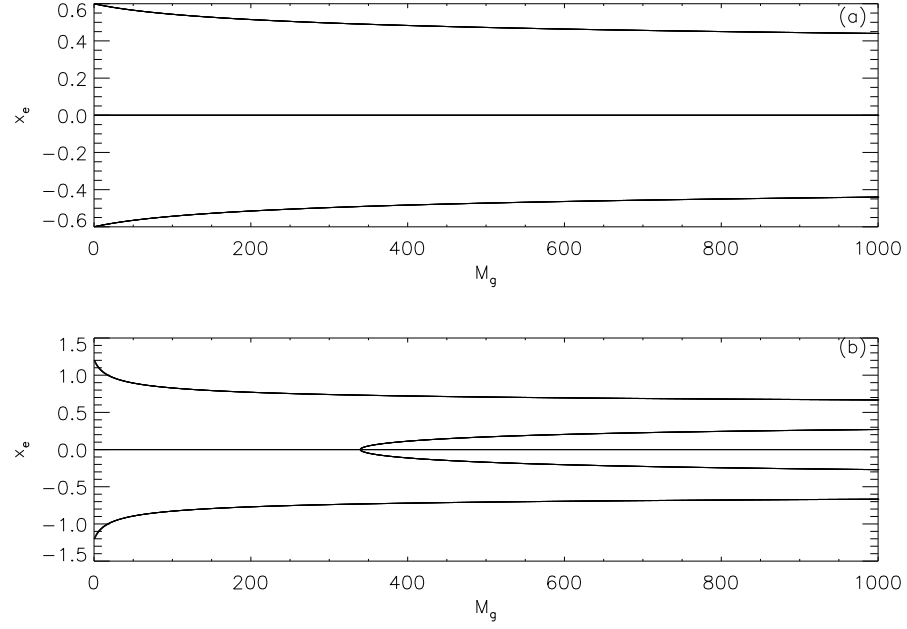


Fig. 4.— The locations of the equilibrium points on the x -axis with $m = 1$ as a function of M_g . (a) is for $R = 0.25$ and (b) is for $R = 0.5$.

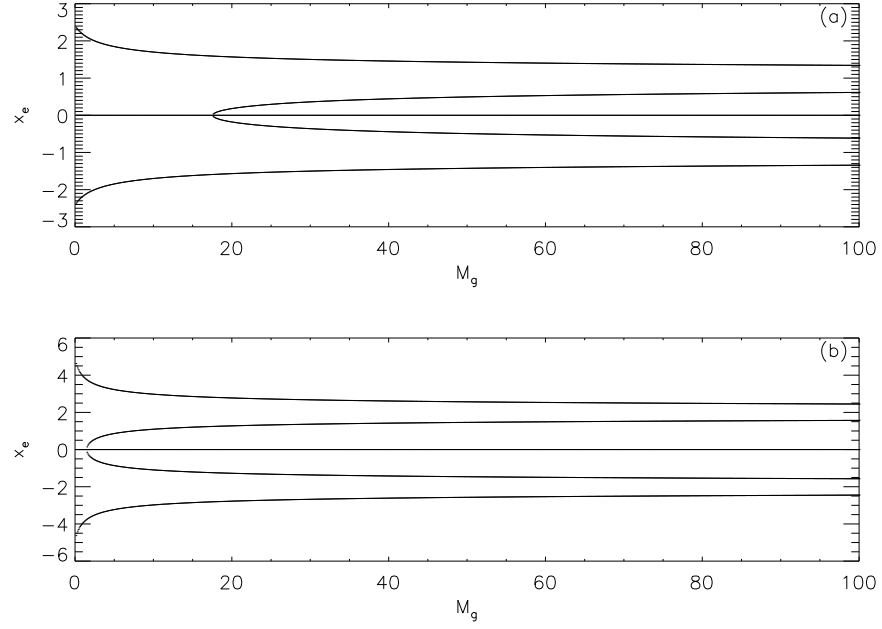


Fig. 5.— The locations of the equilibrium points on the x -axis with $m = 1$ as a function of M_g . (a) is for $R = 1$ and (b) is for $R = 2$.

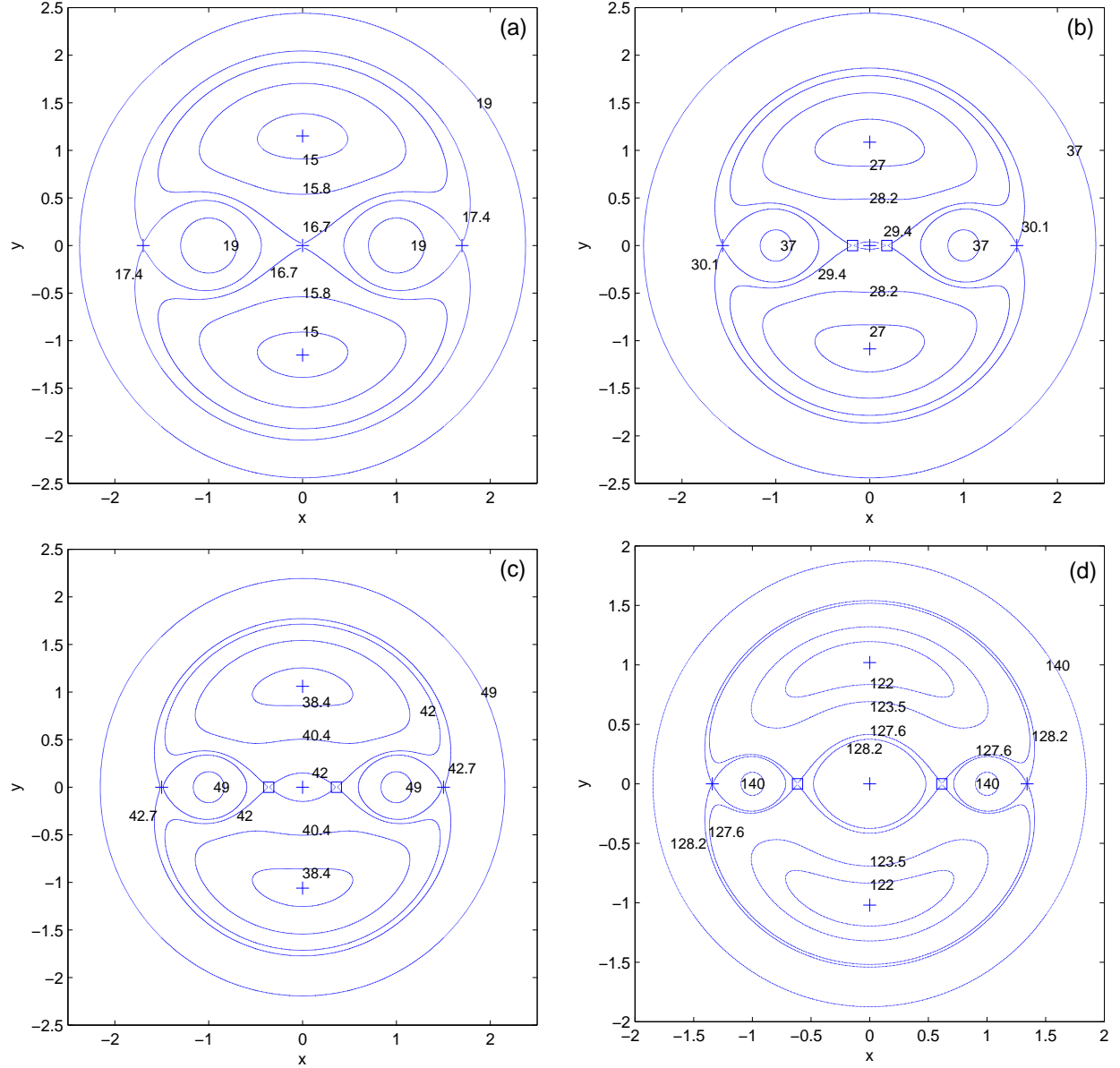


Fig. 6.— The zero-velocity curves of the system when $R = 1$ and $m = 1$, on which the corresponding values of the Jacobi integral C_J are labelled. (a) is for $M_g = 10$, (b) is for $M_g = 20$, (c) is for $M_g = 30$, and (d) is for $M_g = 100$. The + signs indicate the locations of Lagrange Points and the squares indicate the locations of Jiang-Yeh Points.

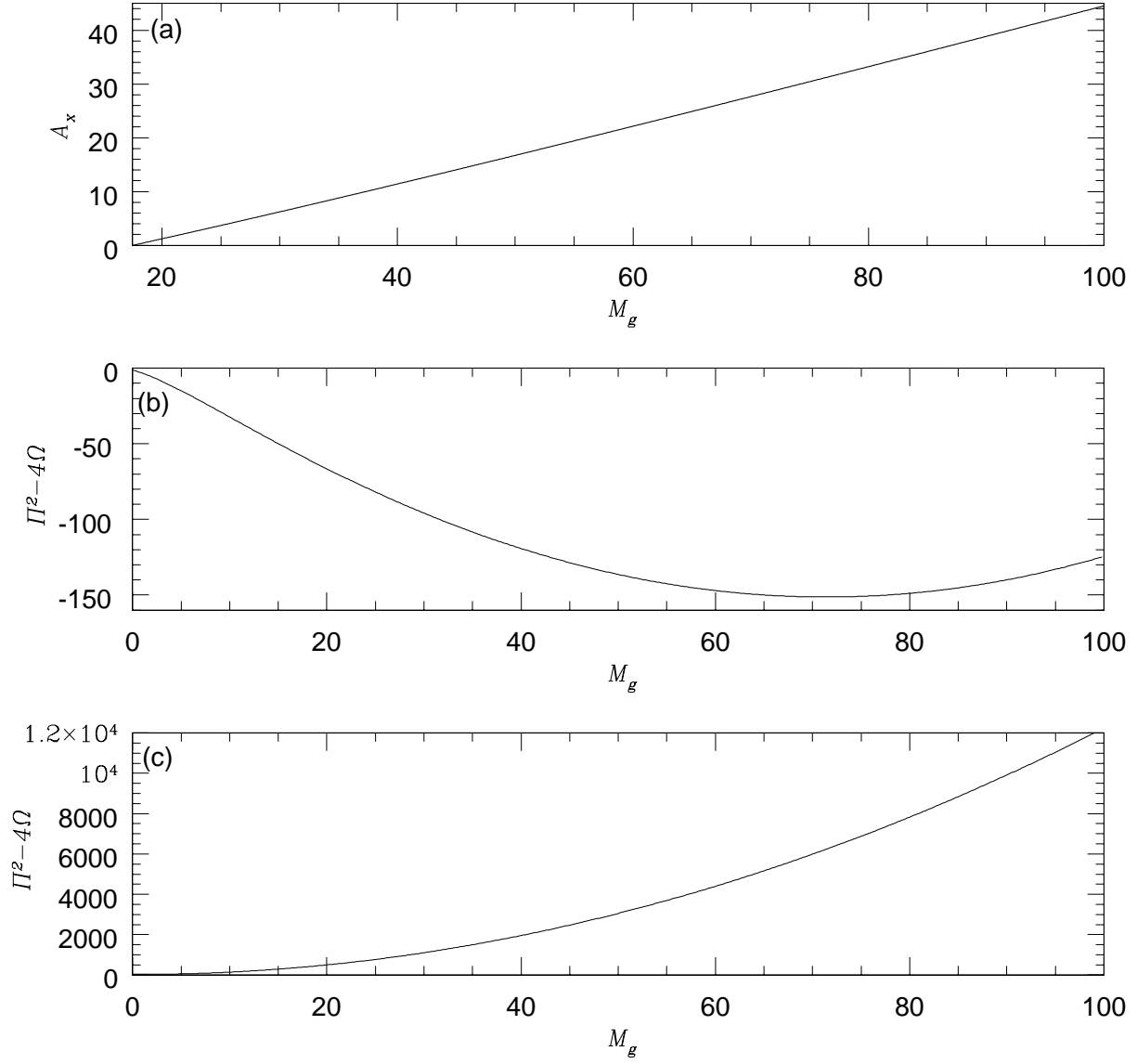


Fig. 7.— (a) The value of A_x as a function of M_g for JY1. (b) $\Pi^2 - 4\Omega$ as a function of M_g for L4. (c) $\Pi^2 - 4\Omega$ as a function of M_g for L1 when $M_g > M_c$.